V International Conference on Computational Methods for Coupled Problems in Science and Engineering
COUPLED PROBLEMS 2013
S. Idelsohn, M. Papadrakakis and B. Schrefler (Eds)

SCHWARZ ALTERNATING DOMAIN DECOMPOSITION APPROACH FOR THE SOLUTION OF MIXED HEAT CONVECTION FLOW PROBLEMS BASED ON THE METHOD OF APPROXIMATE PARTICULAR SOLUTIONS

CARLOS A. BUSTAMANTE*, HENRY POWER† AND WHADY F. FLOREZ†

*Institute of Energy, Materials and Environment
Universidad Pontificia Bolivariana
Circular 1 No 73-34, Medellín, Colombia
e-mail: carlos.bustamante@upb.edu.co, whady.florez@upb.edu.co web page: http://www.upb.edu.co/

†School of Mechanical, Materials and Manufacturing Engineering
University of Nottingham
University Park, Nottingham NG7 2RD, UK
e-mail: henry.power@nottingham.ac.uk - Web page: http://www.nottingham.ac.uk

Key words: Instructions, Coupled Problems, Multiphysics Problems, Applications, Computing Methods

Abstract. The incompressible two-dimensional Navier-Stokes equations including thermal energy balance equation are solved by the recently developed Method of Approximate Particular Solutions (MAPS). In a previous authors' work this method was implemented to solve the two-dimensional Stokes equations by employing the pressure and velocity particular solutions obtained by Oseen's decomposition with the Multiquadric (MQ) RBF as non-homogeneous term. A pressure-velocity linkage strategy is not required since the pressure particular solutions are obtained from the velocity ones. In the present contribution, the Navier-Stokes equations with Boussinesq approximation are solved by linearizing the convective term in a Picard iterative scheme. With the velocity values obtained at each of the Picard iterations, the energy conservation equation is solved by the MAPS by approximating temperature with the particular solutions of a Poisson problem with the MQ as a forcing term. With the aim of improving the computational efficiency of the global strategy, the two-dimensional domain is split into overlapped rectangular subdomains where the Schwarz Alternating Algorithm is employed to find a solution by using velocity and temperatures values from neighbouring zones as boundary conditions. The mixed convection lid-driven cavity flow problem is solved for moderate Reynolds and low Richardson numbers with the aim of validating the proposed method.

1 INTRODUCTION

Mixed natural and forced convection problems are frequently found in industrial applications [1, 2]. Therefore, a detailed understanding of the transport phenomena involved is a key aspect when designing new devices or improving old designs. In this sense, numerical methods for solving partial differential equations (PDEs) have become an interesting tool because they allow obtaining a deterministic description of temperature, pressure and velocity field by solving the momentum and energy conservation equations in their differential form which in case of incompressible fluid problems are known as the Navier-Stokes equations. The accuracy of new numerical methods for solving PDEs ought to be verified by comparing their results to analytical solutions or other tested numerical results. When dealing with non-isothermal flows with mixed convection, the lid-driven cavity flow problem with differentially heated top and bottom walls has widely employed for code verification. Besides validation, several authors analysed the influence of the characteristic dimensionless numbers on the heat transferred through the cavity walls quantified by the Nusselt (Nu) number. For instance, Torrance et al. [3] studied the buoyancy effect on the flow structure by changing the Grashof (Gr) number, while Moallemi and Jang [1] found that the buoyancy effect are more notorious and the heat transfer is higher as the Prandlt (Pr) number is increased. Iwatsu et al. [4] analysed the influence of the Richardson ($Ri = Gr/Re^2$) number in the cavity flow problem based on numerical results. They concluded that for $Ri < 1$ the buoyancy effect is almost neglected and the flow structure is similar to the one found for isothermal flows, while for $Ri > 1$ the buoyancy effect sharply modified the flow structure. More recently, T.S. Cheng [5] studied the relationship between Nu and Pr,Re and Ri in the cavity flow problem. Based on numerical results, the author corrected the correlation proposed by Moallemi and Jang [1] to take into account the sudden decrease in Nu value when increasing Re for $Ri > 1$ due to the change in the flow structure. In the present work some of the results found by the aforementioned authors are employed with the aim of validating a novel meshless strategy based on the Method of Approximated Particular Solutions (MAPS) for the solution of mixed convection problems with the Bousinessq approximation.

Meshless methods have been intensively developed during the last two decades due to its potential characteristics to deal with complex geometry domains without spending too much CPU time in the pre-processing phase. Among the meshless methods, collocation schemes have offered high accuracy as well as versatility to enforce boundary conditions in complex geometries. The Radial Basis Function (RBF) collocation method, originally suggested by Kansa [6], has been successfully used for the solution of several boundary value problems governed by different PDEs. However, it is well known that global RBF collocation methods suffer of a fundamental problem described by Robert Schaback [7] as the uncertainty relation: Better conditioning is associated with worse accuracy, and worse conditioning is associated with improved accuracy. This problem can be mitigated by using integrated RBF approaches such as the indirect RBF (IRBF) collocation method

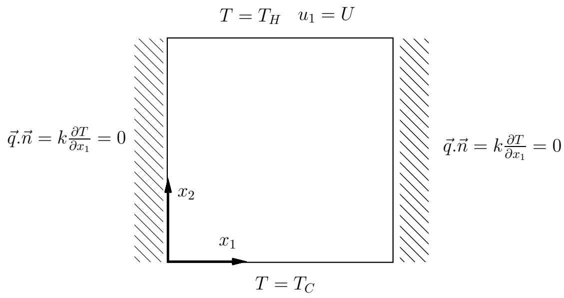

Figure 1: Solution domain and boundary conditions

proposed by Mai-Duy and Tran-CongMay [8] and the Method of Approximate Particular Solutions (MAPS) developed by Chen et al. [9]. In both schemes the RBFs are used to approximate the highest order derivative in the PDE (IRBF) or the complete PDE (MAPS), thus the solution is approximated by an integration process, which unlike derivation does not contain inherent inaccuracy of the approximation.

In previous authors' work [10] a new meshless method for solving the Navier-Stokes equations was developed and used to solve some benchmark flow problems such as the square cavity up to $Re = 3200$ and the backward facing step at $Re = 800$. This approach is based on the Method of Approximate Particular Solutions (MAPS) proposed by Chen et al. [9]. In order to achieve a more efficient strategy without affecting the accuracy obtained with the global method, we employ the Schwartz alternating algorithm as it was originally proposed by Schwarz [11]. This is a suitable option since the MAPS can be employed in its global version to solve the problem in relatively small overlapped subdomains without losing accuracy and preserving its stability in terms of the shape parameter value. The present work is sorted as follows. In the first section the non-isothermal lid-driven cavity flow problem is detailed as well as the governing equations. Then, a brief description of the MAPS for solving scalar and the two-dimensional Navier-Stokes equations is made. Following, the Schwarz Alternating scheme and the decoupling algorithm for solving in sequential way momentum and energy conservation equations are presented. Finally, the numerical results are shown and discussed.

2 PROBLEM DESCRIPTION AND GOVERNING EQUATIONS

The square cavity domain of side L and the problem boundary conditions are shown in Figure 1. The domain is two-dimensional and it is filled with an incompressible fluid. As can be observed the vertical walls are isolated while the horizontal one at the bottom is at temperature T_C and the upper wall is at temperature T_H and moves with horizontal velocity U.

The incompressible steady Navier-Stokes equations in its primitive variable formulation with Boussinesq approximation to take into account the effect of temperature on density, is given by the following equations

$$\frac{\partial u_j}{\partial x_j} = 0 \tag{1}$$

$$\rho u_j \frac{\partial u_i}{\partial x_j} = -\frac{\partial p}{\partial x_i} + \mu \frac{\partial^2 u_i}{\partial x_j \partial x_j} + g_i \beta (T - T_c) \tag{2}$$

$$u_j \frac{\partial T}{\partial x_j} = \alpha \frac{\partial^2 T}{\partial x_j \partial x_j}, \tag{3}$$

which are the mass, momentum and energy conservation equations, with $i = 1, 2$ for two-dimensional problems. The fluid properties ρ, μ, β and α are, respectively, density, absolute viscosity, thermal compressibility coefficient and thermal diffusivity, while $\vec{g}$ refers to the gravity vector and T_C to the lowest temperature in the system. Considering that U and L are the characteristic velocity and length and T_H is the highest temperature, the dimensionless numbers that characterise the situation are $Re = \rho LU/\mu$, $Pr = \mu/\rho/\alpha$, $Gr = |\vec{g}|\rho^2\beta(T_h - T_c)L^3/\mu^2$ and $Ri = Gr/Re^2$. Heat transfer through the top ($b = L$) or bottom ($b = 0$) wall is quantified by the local Nu number, which is defined as

$$Nu(x_1, b) = \frac{1}{T_H - T_C} \left. \frac{\partial T}{\partial x_2} \right|_{\vec{x}=(x_1,b)}, \tag{4}$$

and by its average given by $\bar{Nu} = \int_0^1 Nu(x_1, b) dx_1$

3 METHOD OF APPROXIMATED PARTICULAR SOLUTIONS

The first MAPS version, proposed as a global scheme by Chen et al. [9], is briefly presented in the first part of this section. This version is employed here in order to solve the energy conservation equation (3). In the second part, the proposed MAPS version for solving the isothermal Navier-Stokes equation is presented.

3.1 MAPS for scalar problems

Let us consider the case of a linear boundary value problem whose partial differential operator $L(.(\vec{x}))$, or only part of it, is in terms of the radial component of a polar or spherical coordinate system (i.e. axisymmetric), as:

$$L(u(\vec{x})) = L_r(u(r)) + L_{\vec{x}}(u(\vec{x})) = f(\vec{x}), \tag{5}$$

and

$$B(u(\vec{x})) = g(\vec{x}) \quad \forall \vec{x} \in \Gamma \tag{6}$$

with $L_r(u)$ as the axisymmetric part of the PDE and B as the boundary operator.

The axisymmetric part of the PDE, is approximated by RBFs, as:

$$L_r(u(r)) = \sum_{k=1}^{N} \alpha_k \phi(r_k) \tag{7}$$

where the non-homogeneous term in the momentum equation, ϕ, is defined as the Multiquadric (MQ) RBF, $\phi(r) = (r^2 + c^2)^{1/2}$, which only depends on the Euclidean distance r between a field point $\vec{x}$ and a trial point $\vec{\xi}$ and the shape parameter c. In consequence, the field variable can be expressed as

$$u(\vec{x}) = \sum_{k=1}^{N} \alpha_k \hat{u}(r_k), \tag{8}$$

with $\hat{u}(r)$, as the corresponding particular solution of the following non-homogeneous ordinary differential equation:

$$L_r(\hat{u}(r)) = \phi(r). \tag{9}$$

Thus the complete linear PDE operator can be expressed as a function of the RBFs and the particular solutions in the following way:

$$L(u(\vec{x})) = \sum_{k=1}^{N} \alpha_k \left[\phi(r_k) + L_{\vec{x}}(\hat{u}(r_k))\right] = f(\vec{x}), \tag{10}$$

By substituting the above approximation for $u(\vec{x})$, equation (8), into the boundary conditions of the problem, and into the full expression of PDE, the following linear system of algebraic equations is obtained:

$$\begin{pmatrix} B[\hat{u}_{1,1}] & \cdots & B[\hat{u}_{1,N}] \\ \vdots & \ddots & \vdots \\ B[\hat{u}_{N_b,1}] & \cdots & B[\hat{u}_{N_b,N}] \\ \phi_{N_b+1,1} + L_{\vec{x}}[\hat{u}_{N_b+1,1}] & \cdots & \phi_{N_b+1,N} + L_{\vec{x}}[\hat{u}_{N_b+1,N}] \\ \vdots & \ddots & \vdots \\ \phi_{N,1} + L_{\vec{x}}[\hat{u}_{N,1}] & \cdots & \phi_{N,N} + L_{\vec{x}}[\hat{u}_{N,N}] \end{pmatrix} \begin{pmatrix} \alpha_1 \\ \vdots \\ \alpha_{N_b} \\ \alpha_{N_b+1} \\ \vdots \\ \alpha_N \end{pmatrix} = \begin{pmatrix} g_1 \\ \vdots \\ g_{N_b} \\ f_{N_b+1} \\ \vdots \\ f_N \end{pmatrix} \tag{11}$$

for N_b boundary points and N_i internal points, with $N = N_b + N_i$ and $\hat{u}_{ij} = \hat{u}(\vec{x}_i, \vec{\xi}_j)$. The solution of the boundary value problem is achieved after solving the resulting algebraic system for the coefficients α.

3.2 Solution of the Navier-Stokes equations by MAPS

Before solving the incompressible and isothermal Navier-Stokes equations by the MAPS, the procedure presented in [12] is done in order to obtain the particular solutions $\hat{u}_i^l$ and $\hat{p}^l$ by employing the Oseen's decomposition formula applied to the Stokes problem. In this way, the approximated velocity and pressure fields, $\vec{u}$ and p, can be expressed as a linear superposition of N particular solutions located at N trial points $\vec{\xi}_k$, as:

$$u_i(\vec{x}) = \sum_{k=1}^{N} \alpha_k^l \hat{u}_i^l(r_k) \tag{12}$$

$$p(\vec{x}) = \sum_{k=1}^{N} \alpha_k^l \hat{p}^l(r_k) \tag{13}$$

where $r_k = \left|\vec{x} - \vec{\xi}_k\right|$.

By substituting the above expressions into a linearized version of the momentum equation (2), given by

$$\mu \frac{\partial^2 u_i}{\partial x_j \partial x_j} - \rho u_j^* \frac{\partial u_i}{\partial x_j} - \frac{\partial p}{\partial x_i} = 0, \tag{14}$$

with $\vec{u}^*$ as the solution at the previous iteration of the Picard algorithm, the following homogeneous linear superposing of functions, representing the approximated momentum equation, is obtained:

$$\sum_{k=1}^{N} \alpha_k^l \left[\mu \frac{\partial^2 u_i^l(r_k)}{\partial x_j \partial x_j} - \frac{\partial p^l(r_k)}{\partial x_i} - \rho u_j^* \frac{\partial u_i^l(r_k)}{\partial x_j}\right] = \sum_{k=1}^{N} \alpha_k^l \left[\phi(r_k)\delta_{il} + \Theta_i^l(r_k)\right] = 0, \tag{15}$$

and the last term on the left is

$$\Theta_i^l(r_k) = -\rho u_m^*(\vec{x}) \frac{\partial u_i^l(r_k)}{\partial x_m}. \tag{16}$$

The set of equations required to complete the collocation process is obtained by substituting the approximations (12) and/or (13) into the respective boundary condition. By collocating the resulting expression at the N_b boundary nodes on Γ_u, for each of the components $k = 1, 2$, the first two set of lines on the matrix system (17) are found, while collocation of (15) at the N_i internal nodes, for each of the components $k = 1, 2$, defines the last two set of equations of the matrix system

$$\begin{pmatrix} B^1\left[\hat{u}_1^1, \hat{u}_2^1, \hat{p}^1\right] & B^1\left[\hat{u}_1^2, \hat{u}_2^2, \hat{p}^2\right] \\ B^2\left[\hat{u}_1^1, \hat{u}_2^1, \hat{p}^1\right] & B^2\left[\hat{u}_1^2, \hat{u}_2^2, \hat{p}^2\right] \\ \left[\phi + \Theta_1^1\right] & \left[\Theta_1^2\right] \\ \left[\Theta_2^1\right] & \left[\phi + \Theta_2^2\right] \end{pmatrix} \begin{pmatrix} \left[\alpha^1\right] \\ \left[\alpha^2\right] \end{pmatrix} = \begin{pmatrix} \left[g(\vec{x})_1\right] \\ \left[g(\vec{x})_2\right] \\ [0] \\ [0] \end{pmatrix}, \tag{17}$$

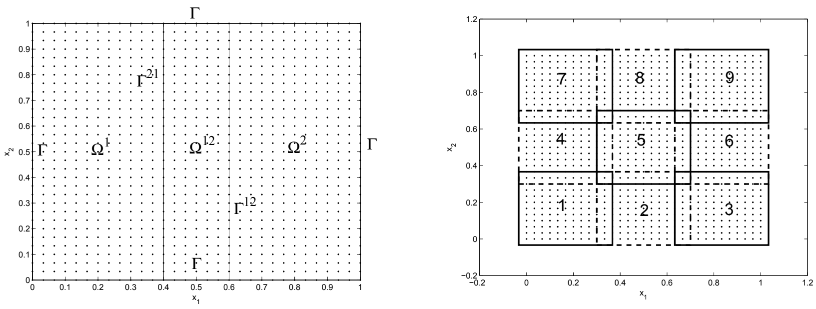

a. b.

Figure 2: Domain decomposition into overlapped subdomains, a. Two subdomains $s = 2$, b. Nine subdomains $s = 9$

where a general form of the boundary condition $B^k\left[u_1, u_2, p\right] = g(\vec{x})_k$, with B^k as the boundary operator and g_k the corresponding value of the boundary condition, was employed. Despite the fact that the continuity equation is not explicitly imposed in the resulting matrix system of equations, the formulation is mass conservative since the used superposition of particular solutions exactly satisfy the continuity equation.

4 SOLUTION ALGORITHMS

In the first part of this section the Schwarz Alternating Method is explained for its application to solve isothermal Navier-Stokes equation. A similar algorithm which is not shown here for brevity is used when solving the energy equation. The decoupled algorithm for solving the PDE system (mass, momentum and energy equations) is then detailed in the second part.

4.1 Schwarz Alternating Method

The Schwarz Alternating Method is a suitable strategy to improve the computational efficiency of the MAPS since local problems can be solved as though it were a global problem which only depends on the neighbouring subdomains by the boundary conditions. Let's suppose a rectangular domain split in two subdomains (Ω^1 and Ω^2) as it is shown in Figure 2a. The original Navier-Stokes problem can be rewritten as follows

$$\rho u_j^* \frac{\partial u_i^k}{\partial x_j} = -\frac{\partial p^k}{\partial x_i} + \mu \frac{\partial^2 u_i^k}{\partial x_j \partial x_j} \quad \forall \vec{x} \in \Omega^k, \tag{18}$$

$$u_i^k = u_{ib} \quad \forall \vec{x} \in \Gamma, \tag{19}$$

where the superscript k refers to the corresponding subdomain. The Schwarz solution is achieved by solving, in first place, the above equations for $k = 1$ and the boundary condition given by $u_i^1 = u_i^2 \quad \forall \vec{x} \in \Gamma^{12}$, then for $k = 2$ and the boundary condition

$u_i^2 = u_i^1 \quad \forall \vec{x} \in \Gamma^{21}$, and so on until the L_2-norm of the difference between successive solutions go less than the specified tolerance. Since we are only dealing with Dirichlet boundary conditions, an additional equation must be solved after solving the Navier-Stokes equations in order to guarantee continuity of pressure throughout the global domain. Regarding pressure particular solution is obtained by integration, the approximated pressure is expressed as:

$$p^m(\vec{x}) = \sum_{k=1}^{N^m} \alpha_k^{lm} \hat{p}^l \left(\left\| \vec{x} - \vec{\xi}_k \right\| \right) + c^m \tag{20}$$

with the superscript $m = 1, 2$ indicating the corresponding subdomain and c^m as the integration constant. The following equation is obtained after evaluating the pressures at some point $\vec{x}_{12}$ in the overlapping zone Ω^{12}:

$$c_2 - c_1 = \sum_{k=1}^{N^1} \alpha_k^{l1} \hat{p}^l \left(\left\| \vec{x}_{12} - \vec{\xi}_k \right\| \right) - \sum_{k=1}^{N^2} \alpha_k^{l2} \hat{p}^l \left(\left\| \vec{x}_{12} - \vec{\xi}_k \right\| \right). \tag{21}$$

The above equation can be solved after fixing the value of one of the integration constants. In case of splitting the domain into more than two subdomains, as shown in Figure 2b for $s = 9$ with s as the number of subdomains, the solution is obtained by solving the problem given by equations (18) to (19). In this case the superscript k changes in the sequential order shown in Figure 2b and the solution $k+1$ is obtained by using the boundary conditions with the variable value available in memory either after obtaining a solution for the $j = 1, \ldots, i-1$ subdomains or as the initial value in the first Schwarz iteration. The matching equation for pressure (21) becomes an overdetermined equation system with $s-1$ variables (integration constants) and one equation for each overlapped zone in the domain. For better understanding of the Schwarz scheme, the algorithm employed for solving a generic PDE with dependent variable ϕ is presented:

- After setting an initial guess $\phi^0(\vec{x})$, compute the interpolation matrix on the left hand side of equation (17) when solving the Navier Stokes equations or (11) in case of scalar problems, for each of the s subdomains.

- For each subdomain ($l = 1, \ldots, s$) calculate the column vector on the RHS of equation (17) or (11) with the variable values available in memory and solve the equation system to obtained α coefficients.

- For each subdomain ($l = 1, \ldots, s$) reconstruct ϕ and store its value in memory

- Evaluate the L_2-norm of the difference between the values of the variable ϕ at the present and previous Schwarz iterations ($||\phi^n - \phi^{n-1}||$). If it is less than or equal to the set tolerance tol_{sc}, for all of the variables, stop the Schwarz algorithm, if not go to the second step with $\phi^{n-1} = \phi^n$.

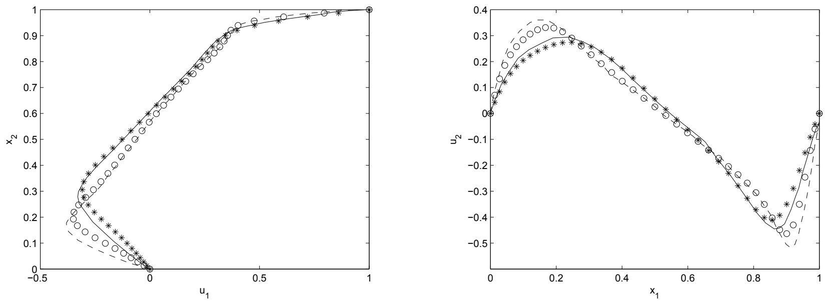

a. b.

Figure 3: Velocity profiles for $Gr = 100$ and $Re = 400(*)$ and $Re = 1000(\circ)$ in comparison to the numerical solution reported by Iwatsu et al. [4], a. u_1 velocity on $x_1 = 0.5$, b. u_2 velocity on $x_2 = 0.5$

4.2 Sequential solution procedure

The following algorithm is implemented for solving in a decoupled way the equations 1,2 and 3:

- By using the MAPS as explained in section 2.2, solve the following form of the momentum equation in order to obtain the fields $\vec{u}^k$ and p^k based on the guess (first iteration) or the previous iteration variable values $\vec{u}^{k-1}$ and T^{k-1}

$$\mu\frac{\partial^2 u_i^k}{\partial x_j \partial x_j} - \rho u_j^{k-1}\frac{\partial u_i^k}{\partial x_j} - \frac{\partial p^k}{\partial x_i} = g_i \rho\beta(T^{k-1} - T_c). \tag{22}$$

- By employing the MAPS for scalar problems (section 2.1) and with the velocity obtained in the previous step, solve the following form of the energy equation in order to obtain the updated temperature value (T^k)

$$\alpha\frac{\partial^2 T^k}{\partial x_j \partial x_j} - u_j^k\frac{\partial T^k}{\partial x_j} = 0. \tag{23}$$

- If $\left\|\phi^k - \phi^{k-1}\right\| < tol_{pi}$ for all $\phi = \vec{u}$,p,T, stop, if not make $\phi^{k+1} = \phi^k$ and go to the first step.

5 NUMERICAL RESULTS

Numerical results were obtained for $Re = 400$, 1000 and $Gr = 1 \times 10^2$, 1×10^4 with a 41×41-point nodal distribution refined towards the boundaries and $c = 0.01$ for velocity and temperature approximation. Besides, the domain is split into $s = 4 \times 4$ overlapped subdomains in order to applied the Schwarz alternating algorithm. As shown in Table 1, the mentioned dimensionless numbers were achieved by combining some values of the fluid

Table 1: Properties and Dimensionless number values for the solved cases

Quantity	Case 1	Case 2	Case 3	Case 4
$\rho\ (kg/m^3)$	4.00×10^2	4.00×10^2	1.00×10^3	1.00×10^3
$\beta\ (1/^oC)$	6.25×10^{-5}	6.25×10^{-3}	1.00×10^{-5}	1.00×10^{-3}
$\alpha\ (m^2/s)$	3.52×10^{-3}	3.52×10^{-3}	1.41×10^{-3}	1.41×10^{-3}
Re	4.00×10^2	4.00×10^2	1.00×10^3	1.00×10^3
Gr	1.00×10^2	1.00×10^4	1.00×10^2	1.00×10^4
Ri	6.25×10^{-4}	6.25×10^{-2}	1.00×10^{-4}	1.00×10^{-2}

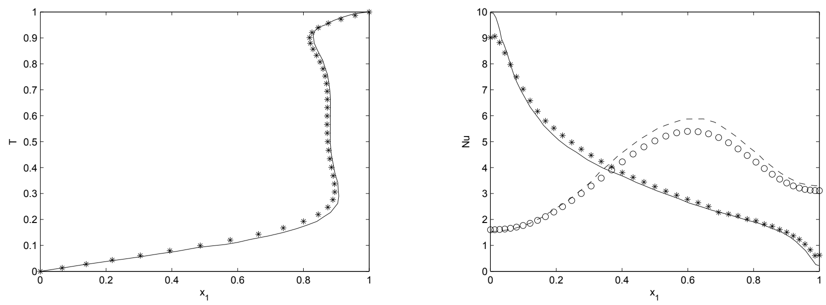

a. b.

Figure 4: Numerical results for $Gr = 100$ and $Re = 400$ in comparison to the numerical solution reported by Iwatsu et al. [4], a. T on $x_1 = 0.5$, b. Nu on $x_2 = 0.0$ ($\circ$) and $x_2 = 1.0$ ($*$)

properties since boundary conditions different to zero were fixed as the unity, i.e. $U = 1$ and $T_H = 1$. The fixed properties were $\mu = 1kg/m/s$, $Pr = 0.71$ and $\vec{g} = (0, -10)m/s^2$.

In Figure 3, the obtained velocity profiles are compared to the ones attained by Iwatsu et al. [4]. Numerical results are in good agreement to the reference solution regarding that the nodal distribution used here (41×41) is coarser than the one used by Iwatsu et. al (128×128). For $Re = 400$ and 1000 and $Gr = 100$, the buoyancy effect is not predominant since Richardson numbers are, respectively, $Ri = 6.25 \times 10^{-4}$ and $1.00 \times^{-4}$, which are much less than the unity. Therefore, the velocity field is close to the isothermal pattern. Despite of the coarseness of the nodal distribution employed, accurate results were found for temperature (Figure 4a) and the local Nu on the bottom and top boundaries (Figure 4b). Since local Nu is calculated based on the temperature derivatives, it is not as accurate as temperature profile, increasing the difference towards the corners in the case of the top boundary profile and near to the centre for the bottom boundary. Nevertheless, the highest difference between the obtained and the reference average Nu values, presented in Table 2 for the top boundary, are 2.54% and 9.42% when comparing to the results reported in [4] and [5], respectively. By using the aforementioned solution algorithm, the highest Ri values achieved before the Picard iterations diverge, were $Ri = 6.25 \times 10^{-2}$ and 1.00×10^{-2} with $Re = 400$ and 1000 ($Gr = 1 \times 10^4$), respectively. In consequence,

Table 2: Average Nusselt number on top boundary

Re	Reference	Grid	Gr	
			1×10^2	1×10^4
400	Iwatsu et al. [4]	128×128	3.84	3.62
	Cheng [5]	128×128	4.14	3.90
	Present	41×41	3.75	3.63
1000	Iwatsu et al. [4]	128×128	6.33	6.29
	Cheng [5]	128×128	6.73	6.68
	Present	41×41	6.20	6.13

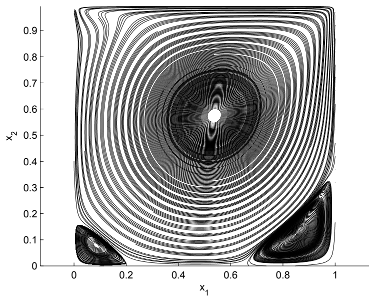

a.

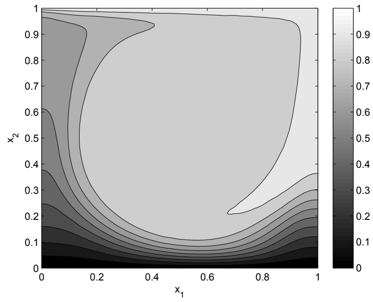

b.

Figure 5: Approximated streamlines (a.) and temperature contours (b.) for $Gr = 1 \times 10^4$ and $Re = 1000$

the approximated streamlines and the temperatures contours, shown for $Re = 1000$ in Figure 5, present a forced convection-dominated behaviour since the buoyancy effect is not notorious. The flow structure and temperature contours are in good agreement with the results reported by Moallemi and Jang [1] in their Figure 2.

6 CONCLUSIONS

- The Method of Approximate Particular Solutions in conjunction to the Schwarz alternating algorithm were used to solve the two-dimensional mixed heat convection lid-driven cavity flow problem at $Re = 400$ and $Re = 1000$ for low Ri. The obtained results are in good agreement to the ones reported in literature, despite the nodal distributions used are much coarser than the ones employed by the reference authors.

- Future authors' work will be focused on obtaining results for higher Ri both by using denser nodal distribution and by implementing a more stable algorithm for the decoupled solution of the momentum and energy conservation equations.

REFERENCES

[1] Moallemi, M. K. and Jang, K. S. Prandtl number effects on laminar mixed convection heat transfer in a lid-driven cavity. *Int. J. Heat Mass Transfer* (1992) **35**:1881–1892.

[2] Cheng, T. S. and Liu, W.-H. Effect of temperature gradient orientation on the characteristics of mixed convection flow in a lid-driven square cavity. *Comput. Fluids* (2010) **39**:965–978.

[3] Torrance K., Davis, R., Eike, K., Gill, D., Gutman, D., Hsui, A., Lyons, S. and Zien, H. Cavity flows driven by buoyancy and shear. *J. Fluid Mech* (1993) **36**:1601–1608.

[4] Iwatsu R., Hyun, J. M. and Kuwahara, K. Mixed convection in a driven cavity with a stable vertical temperature gradient. *Int. J. Heat Mass Transfer* (1972) **51**:221–231.

[5] Cheng, T. S. Characteristics of mixed convection heat transfer in a lid-driven square cavity with various Richardson and Prandtl numbers. *Int. J. Therm. Sci.* (2011) **50**:197–205.

[6] Kansa, E.J. Multiquadrics -a scattered data approximation scheme with applications to computational fluid dynamics-II solution to parabolic, hyperbolic and elliptic partial differential equations. *Comput. Math. Appl.* (1990) **19**:127–145.

[7] Schaback, R. Multivariate interpolation and approximation by translates of basis functions. *Approximation Theory VIII: Wavelets and Multilevel Approximation* (1995) **8**:1–8.

[8] Mai-Duy and N. and Tran-Cong, T. Numerical solution of diferential equations using multiquadric radial basis function networks. *Neural Networks* (2001) **14**:185–199.

[9] Chen, C.S., Fan, C.M. and When, P.H. The method of approximated particular solutions for solving certain partial differential equations. *Numer. Method. Part D. E.* (2012) **28**:506–522.

[10] Bustamante, C.A., Power, H. and Flórez, W.F. A global meshless collocation Particular Solution Method for solving the two-dimensional Navier-Stokes system of equations. *Comp. Math. Appl.* (2013) **under review**:-.

[11] Lions, P. L. On the Schwarz Alternating Method I. *First International Symposium on Domain Decomposition Methods for PDEs* (1998) **1**:1–42.

[12] Bustamante, C.A., Power, H., Sua, Y. H. and Flórez, W. F. A global meshless collocation particular soltuion method (integrated Radial Basis Function) for two-dimensional Stokes flow problems. *Appl. Math. Model.* (2013) **37**:4538-4547.